12-1-2010

Electrochemical Investigation of Azurin Thermodynamic and Adsorption Properties at Monolayer-Protected Cluster Film Assemblies – Evidence for a More Homogeneous Adsorption Interface

Tran Doan

Morgan Lynn Vargo

John K. Gerig

Chris P. Gulka

Matthew L. Trawick
University of Richmond, mtrawick@richmond.edu

See next page for additional authors

Recommended Citation

T. Doan,* M.L. Vargo,* J.K. Gerig,* C.P. Gulka,* M.L. Trawick, J.D. Dattelbaum and M.C. Leopold, "Electrochemical Investigation of Azurin Thermodynamic and Adsorption Properties at Monolayer-Protected Cluster Film Assemblies-Evidence for a More Homogeneous Adsorption Interface," *J. of Colloid and Interface Science* 2010, *352*, 50-58.

For submission to Journal of Colloid and Interface Science

Electrochemical Investigation of Azurin Thermodynamic and Adsorption Properties at Monolayer-Protected Cluster Film Assemblies – Evidence for a More Homogeneous Adsorption Interface

Tran Doan,[†] Morgan L. Vargo,[†] John K. Gerig, Chris P. Gulka, Matthew L. Trawick[‡], Jonathan D. Dattelbaum, and Michael C. Leopold*

Department of Chemistry, Gottwald Center for the Sciences, University of Richmond Richmond, VA 23173

[‡]*Department of Physics, Gottwald Center for the Sciences, University of Richmond Richmond, VA 23173*

Abstract

Thermodynamic and adsorption properties of protein monolayer electrochemistry (PME) are examined for *Pseudomonas aeruginosa* azurin (AZ) immobilized at an electrode modified with a networked film of monolayer protected clusters (MPCs) to assess if nanoparticle films of this nature offer a more homogeneous adsorption interface compared to traditional self-assembled monolayer (SAM) modified electrodes. Specifically, electrochemistry is used to assess properties of surface coverage, formal potential, peak broadening, and electron transfer (ET) kinetics as a function of film thickness. The modification of a surface with dithiol-linked films of MPCs ($Au_{225}C6_{75}$) provides a more uniform binding interface for AZ that results in voltammetry with less peak broadening (<110 mV) compared to SAMs (>120-130 mV). Improved homogeneity of the MPC interface for protein adsorption is confirmed by atomic force microscopy imaging that shows uniform coverage of the gold substrate topography and by electrochemical analysis of film properties during systematic desorption of AZ, which indicates a more homogeneous population of adsorbed protein at MPC films. These results suggest MPC film assemblies may be used in PME to provide greater molecular level control of the protein adsorption interface, a development with applications for strategies to study biological ET processes as well as the advancement of biosensor technologies.

Keywords: nanoparticle, monolayer-protected clusters, film assemblies, protein monolayer electrochemistry, azurin, self-assembled monolayers, voltammetry, peak broadening, homogeneous interface

---

* To whom correspondence should be addressed. Email: mleopold@richmond.edu. Phone: (804) 287-6329. Fax: (804) 287-1897

† These authors contributed equally to this work.

1. Introduction

Many research interests in the field of bioanalytical chemistry require a fundamental understanding of the interactions between biomolecules and synthetic materials. Of practical interest to biosensor engineering[1-5], biological electron transfer modeling systems[6], and the development of biocompatible materials[7] is the ability to design a uniform adsorption environment across a large surface area for protein adsorption. Developing man-made adsorption platforms and understanding the interfacial protein interactions are popular research topics, including previous research focused on the electrochemistry of redox active proteins at modified electrodes[8-10]. The focus of bioanalytical research in this area is to understand protein interactions at biocompatible materials for applications such as amperometric biosensors, and their miniaturization and implantation for potential *in-vivo* sensors[1-4].

Protein monolayer electrochemistry is the traditional technique for studying electrochemical properties of adsorbed proteins by confining a monolayer of protein to an electrode surface, which also serves as a redox partner. The adsorption of protein on a substrate mimics protein/protein interactions[11, 12], and therefore serves as an appropriate model for studying protein adsorption processes and monitoring changes in the immobilized proteins' structure and function. Alkanethiol self-assembled monolayer (SAM) modified electrodes provide a highly ordered interfacial environment that sustains protein electroactivity, provides a great degree of control over the binding chemistry at the protein/electrode interface[13, 14], and provides discrimination against the background charging current, which can obscure a Faradaic response and complicate voltammetric peak analysis. A wealth of research involving SAM modified electrodes has been performed with cytochrome c (cyt c) by the Bowden[14, 15], Waldeck[2], Niki[16, 17], and Gray groups[17], with azurin (AZ) by Martin[18], Ulstrup[19]

and Niki[20, 21], and by Zapien's group with ferritin[22]. All this research supports the PME technique for studying adsorption and electrochemical behavior of immobilized proteins, where voltammetric experiments are used to report thermodynamic and kinetic properties, such as formal potential, surface coverage, and an electron transfer (ET) rate constant.

However, there are many issues with SAM modified electrodes used in PME because the rigid structure of SAMs mirrors defects in the substrate topography and heterogeneous adsorption sites result in voltammetric peak distortion[23]. Electrochemical theory of adsorbed species predicts voltammetric peak full-width-at-half-maximum (FWHM) values of 90 mV[24]. Bowden examined sources of non-ideality and suggested that a heterogeneous protein population at the SAM interface is a major contributor to deviations from ideal electrochemical theory[25]. Bowden and Clark study the effects of submonolayer protein coverage on the electrochemical parameters, formal potential, electron transfer rate constant, and FWHM. Through stepwise desorption of cyt c from a 16-MHDA/Au substrate with increasing buffer strength Bowden and Clark show that submonolayer voltammetric peaks are narrower and more ideal, as a decrease in formal potential and an increase in the ET rate occur with decreasing protein surface coverage[25].

More ideal PME voltammetry is dependent on engineering an interface that provides a uniform adsorption environment and negates substrate topography[23, 25]. Many researchers have recognized the advantages of nanoparticles (NPs) in potential biosensor designs including a large surface-to-volume ratio that yields greater protein adsorption, increased freedom of orientation for adsorbed biomolecules, preservation of electroactivity of adsorbed molecules, the ability to act as conductive pathways for ET reactions, and the ability to manipulate core size and peripheral functionalization for greater protein adsorption[26][27]. In a previous report, Leopold

has shown that nonaqueous alkanethiol-protected NPs, known as Monolayer-Protected Clusters (MPCs), as a component of PME provide molecular level control of the interface and affect cyt c adsorption and electrochemistry[28]. In this study, particular attention was given to film composition to ensure preservation of the signal to background ratio despite the higher dielectric of the NP material. Leopold has previously studied AZ ET kinetics as a function of MPC film structure and extensively characterized the MPC film with verification of film thickness. Thick MPC films show no distance dependence for ET kinetics, which is especially advantageous for PME biosensors of higher order architecture and studies of electron transfer processes[29].

Earlier research done by the Leopold group[28, 29] has led to this report, where we more extensively examine the thermodynamics and adsorption properties of AZ electrochemistry at MPC film assemblies compared to the traditional PME platforms of SAMs. Specifically, we investigate if the use of an MPC film provides a more homogeneous electrode-solution interface that enables adsorption of a more uniform protein population. In this work, we continue our focus on the copper blue redox protein AZ, as it allows us to greatly simplify the binding interface of the MPC film. Voltammetry-based measurements of AZ surface coverage, formal potential, peak shape, ET kinetics, as well as controlled desorption experiments applied to AZ adsorbed to both SAM and MPC platforms suggest that MPC films indeed provide a more homogeneous surface environment for protein adsorption over a large surface area. This finding is significant for biosensor design and biocompatible materials, which incorporate nanomaterials that require higher order interfacial control for specific protein adsorption.

2. Experimental Section

2.1. Chemicals and Materials

1-butanethiol (C4), 1-hexanethiol (C6), 1-octanethiol (C8), 1-decanthiol (C10), 1-dodecanethiol (C12), 1-tetradecanethiol (C14, Fluka), 1-hexadecanethiol (C16), 1-octadecanethiol (C18), 1,9-nonanedithiol (NDT), 1,16-hexadecanedithiol, 11-mercaptoundecanoic acid (MUA), and 6-mercaptohexanoic acid (MHA) were purchased from Sigma-Aldrich and used as received, except for the C14 as noted from Fluka. All aqueous solutions and buffers were made with 18 MΩ ultrapurified (UP) water. For SAM assembly, the thiols were used as 5 mM ethanol (EtOH) solutions. The gold electrode substrate was incubated with the thiol solution for ≥ 24 hours then rinsed with ethanol and used further as described below (thiols longer than a C12 were allowed 48 hours).

As in our prior studies[29], *Pseudomonas aeruginosa* azurin (AZ) was provided by a colleague at the University of Richmond, Dr. Jonathan Dattelbaum, as a purified and lyophilized powder that was rehydrated into aqueous solution prior to use. For quality control, periodic electrochemical testing of the AZ at octanethiol self-assembled monolayers was performed to monitor changes in formal potential, surface coverage, or rate constant over time. The original plasmid for the protein was graciously provided by Dr. Corey Wilson of Rice University and both production and purification of AZ were conducted as previously described[29].

2.2. Electrochemistry

Electrochemical measurements of double-layer capacitance and cyclic voltammetry were accomplished with CH Instruments potentiostats (model 650A or 610B) with both a low current amplifier and a Faraday cage. The electrochemical sandwich cell used by our group was previously described[28]. Briefly, the cell included a Ag/AgCl (saturated KCl) reference electrode (Microelectrode, Inc.), a platinum wire (Sigma-Aldrich) counter electrode, and an

evaporated gold substrate (EMF Corp., Ithaca, NY) as a working electrode. During typical measurements, the cell was filled with a 4.4 mM potassium phosphate buffer (KPB) (pH=7, μ=10 mM) electrolyte solution and housed in the Faraday cage. The Viton O-ring of the cell defined the a geometric surface area of 0.32 cm^2 on the gold working electrode.

2.3. MPC Synthesis.

Hexanethiolate-protected MPCs were synthesized from gold salt HA_uCl_4, previously crystallized from aqua-regia reflux of 99.99% gold shot, by using the well-established Brust reaction to yield an average structure of $Au_{225}(C6)_{75}$[30, 31]. An aqueous solution of $HAuCl_4$ was treated with tetraoctylammonium bromide in toluene to phase transfer the gold to the nonaqueous layer. Hexanethiol in a ratio of 2:1 with the gold salt was added to the nonaqueous layer, which was stirred for at least 30 minutes to form the Au(I) polymer, as detected by a color change from reddish orange to pale yellow. After chilling the reaction flask in an ice bath for 30 minutes, an aqueous solution of sodium borohydride (~0.5 M) was added to reduce Au(I) to a metallic gold in the presence of thiols, forming a thick black solution of MPCs in toluene. The reaction was stirred overnight, separated, and the toluene was rotary evaporated off to dryness. MPCs were collected as a precipitate in acetonitrile (ACN) using a glass frit of medium porosity. Specific modifications to the Brust reaction, like the specific thiol-to-gold ratios, temperature, and reaction delivery rate, facilitated the production of MPCs with an *average* core composition of Au_{255} and diameter of 2.03 ± 0.95 nm as verified with TEM imaging[29].

2.4. MPC Film Assembly.

MPC films were assembled on evaporated gold substrates (Evaporated Metal Films) based on a procedure previously described[28, 29]. In the MPC film assembly procedure, gold substrates served as the working electrodes when mounted in electrochemical sandwich cells[28, 32]. The gold substrates were electrochemically cleaned[33] in a solution of 0.1 M H_2SO_4 and 0.01 M KCl prior to exposure to a 5 mM hexanethiol solution in ethanol (EtOH) to form an initial SAM. The SAM-modified gold was rinsed consecutively with ETOH and UP water, and then treated with a 5 mM solution nonanedithiol (NDT) in EtOH, the linker ligand, for 1 hour. The gold electrodes were rinsed successively with EtOH, UP water, and methylene chloride (CH_2Cl_2) prior to exposure to a solution of hexanethiolate-protected MPCs dissolved in CH_2Cl_2 (~1 mg/mL), which was bubbled under nitrogen gas for 1 hour in order to successfully anchor the first dithiol-linked MPC layer to the gold electrode. The terms "dip cycle" referred to the process of the successive exposure of substrate to a solution of NDT linking ligands in CH_2Cl_2 and then to the solution of C6 MPC in CH_2Cl_2 with intermittent rinsing with CH_2Cl_2. Beyond the first initial exposure of the gold surface, dip cycles were repeated to make MPC films of varying thickness. The development of the film was monitored with electrochemical measurements of double-layer capacitance as described in the film characterization section.

2.5. Film Characterization and Protein Monolayer Electrochemistry.

As in prior studies, MPC film growth on gold substrates was monitored with double-layer capacitance (C_{dl}) measurements taken of the film system by running cyclic voltammetry in a potential window from 0.1 to 0.4 V (vs. Ag/AgCl, KCl) at 100 mV/s in 4.4 mM potassium phosphate buffer[28, 29]. C_{dl} measurements were used to confirm SAM deposition where a significant decrease in the capacitance, compared to cleaned bare gold, is observed upon self-

assembly. Similarly, we have shown MPC deposition after each MPC dip cycle is accompanied by increasing capacitance with each exposure to MPC solution. The thickness of these MPC film assemblies was the focus of prior work[28, 29], where ellipsometry and cross-sectional TEM were used to characterize film thickness. This worked established that these films grow at ~2.5 nm/dip (i.e., submonolayers of MPC/dip) and have an overall thickness for a 5 dip cycle of ~12.5 nm[29].

After the film assembly's final exposure to the MPC solution, the cell was rinsed with CH_2Cl_2 and then with 4.4 mM potassium phosphate buffer (KPB). Protein was adsorbed to the film assembly by injecting 200 μL of ~5-10 μM AZ in KPB (pH = 7.0, μ= 10 mM) into the cells, followed by refrigeration for 1 hour (6-7 ºC). Cells were allowed to come to near room temperature and rinsed with copious amounts of KPB (pH = 7.0, μ= 10 mM). Protein electrochemical studies were run in the potential window of +0.25 to - 0.25 V at 100 mV/s in supporting electrolyte 4.4 mM KPB (pH = 7.0, μ= 10 mM), which was previously degassed with N_2 for 10 minutes. The surface concentration of AZ (Γ) was determined by integrating the voltammetric peaks with calculations using $Q=nFA\Gamma$ where Q is the charge passed the result of peak integration, n is the number of electrons involved in the ET process, F is Faraday's constant, and A is the defined electroactive area. The electron transfer rate constants (k^o_{ET}) were obtained by using Laviron's simplest model for an adsorbed species. Chiefly, a series of voltammograms were collected at increasingly faster sweep rates to achieve quasi-reversible peak splitting (≤200 mV)[14, 34, 35].

2.6. Microscopy

Transmission electron microscopy (TEM) images of C6 MPC samples were obtained by a JEOL 1010 microscope operating at 80-100 kV. MPC materials, dissolved in toluene, were drop-casted onto 400 mesh copper grid coated with Formvar (Electron Microscopy Sciences). Image analysis was performed using Image J software to determine average core size and polydispersity of the samples[28, 29].

Atomic Force Microscopy images were taken of the evaporated gold substrates on mica (Agilent-Molecular Imaging), which were previously immersed in piranha solution (a 2:1 mixture of concentrated H_2SO_4 and 30% H_2O_2) for 10 minutes to remove all nonaqueous material. *Warning: Extreme caution should be used when handling piranha solution, since it reacts violently with organic material*. Prior to imaging with an AFM the gold/mica substrates were cleaned by rinsing with UP water and drying with a stream of N_2. After imaging the bare substrate, a SAM was prepared on the Au/mica sheets by immersing them in a solution of C6 thiol in EtOH for 3 hours. The substrates were treated with a solution of NDT in EtOH for 20 minutes, followed by a solution of C6 MPCs in CH_2Cl_2, which was stirred by N_2 bubbles for 1hour. This step was repeated, with extensive CH_2Cl_2 rinsing in between exposures for multiple layer deposition of MPC films for about 3-4 cycles. After the final cycle, the sheets were rinsed with CH_2Cl_2 and mounted on glass microscope slides for AFM imaging, which was performed on an MFP-3D microscope from Asylum Research in noncontact (AC) mode. SSS-NCRH SuperSharpSilicon of AFM tips (nominal frequency f_0 = 330 kHz, typical tip radius of curvature 2 nm) were used from Nanosensors. Typical 1μm^2 images were scanned at 0.5 Hz with free-air amplitude $A_0 = 0.30$ V and set point amplitude $A_0 = 0.23$ V[29].

3. Results and Discussion

3.1 Thermodynamic and Electrochemical Properties of Adsorbed Azurin

It has been clearly established that protein monolayer electrochemistry (PME) can be successfully employed to analyze the electrochemistry of azurin (AZ) adsorbed at either self-assembled monolayer (SAM) platforms or monolayer protected cluster (MPC) film assemblies, both of which offer the necessary hydrophobic interactions to bind AZ at the hydrophobic pocket inherent to its structure[28, 36, 37]. In the former system, methyl-terminated SAMs comprised entirely of straight chain alkanthiolates can be readily applied to a gold electrode and, in the latter nanoparticle system, a networked film of dithiol-linked hexanethiolate (C6) MPCs have proven to be an effective combination for AZ immobilization and electrochemistry. Indeed, **Figure 1** present nearly identical cyclic voltammograms of AZ at both a SAM (C6) as well as a

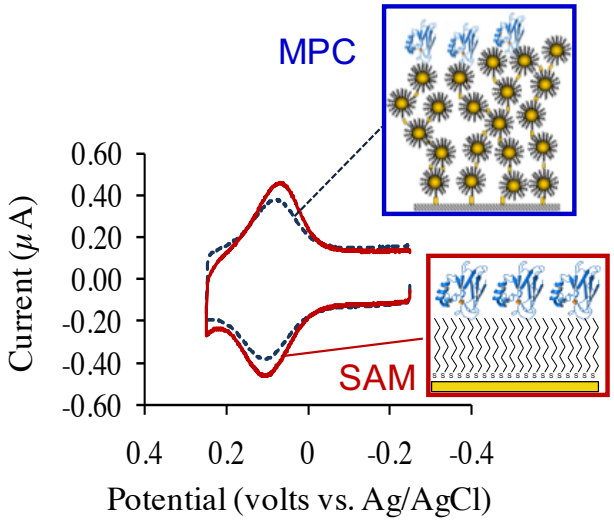

Figure 1. Cyclic voltammograms (100 mV/sec) of azurin monolayers adsorbed to a C6 SAM (solid line, red) and a three layer MPC film composed of $Au_{225}C6_{75}$ (dotted line, blue). Inset: Schematic representations of the systems investigated in this study. [Protein monolayer electrochemistry solution conditions: 4.4 mM potassium phosphate buffer, pH=7, μ=10 mM]

MPC film assembled with three layers of $Au_{225}(C6)_{75}$ MPCs with nonanedithiol (NDT) interparticle linkages. Discrimination of non-faradaic charging currents or background is a key element in both systems that require consideration during film construction. For SAMs of

increasing chainlength, there is a direct corresponding decrease in the double layer capacitance (C_{dl}) of the system as the film thickness increases and the dielectric constant of that barrier decreases to ~2.6, an estimated value similar to other reports on SAM electrochemistry (Supporting Material)[38]. While very dependent on the linking mechanisms within the film, the charging current of the MPC assemblies is known to increase with the number of MPC layers. However, the voltammetry of both types of systems (Figure 1) can be readily observed, is highly repeatable, and is stable for days[28, 29].

Upon the adsorption of AZ to these two different platforms, traditional electrochemical and thermodynamic properties of the protein such as surface coverage (Γ) and formal potential (E°´) were evaluated and compared as a function of respective film thickness – SAMs in terms of the number of methylene units (n, CH_2) in their alkanethiol constituents and MPC films in terms of the number of layers of MPC separating the electrode and the adsorbed AZ. **Figure 2** illustrates the measured results for AZ surface coverage calculated from the integrated voltammetric peak area or charge passed as previously described in the Experimental Section. Of note in both sets of results is the relatively low dependence on film thickness for most of the films tested. AZ surface coverage at most of the SAM modified interfaces was measured as approximately 10-12 pmol/cm^2, consistent with a monolayer or more of adsorbed protein in similar PME studies[18, 20], before a sudden decrease in apparent surface coverage at the longest SAM chainlength (C18 or 17 methylene units) is observed as illustrated in **Figure 2A**. For all of the AZ-SAM systems studied, the average surface coverage was determined to be 11.1 $_{(\pm 3.0)}$ pmol/cm^2.

While there is a slightly lower overall surface coverage for AZ at MPC films, the amount of adsorbed protein is still consistent with reports of near monolayer protein adsorption and is also relatively independent of film thickness up to six layers of MPC (**Figure 2B**). The overall

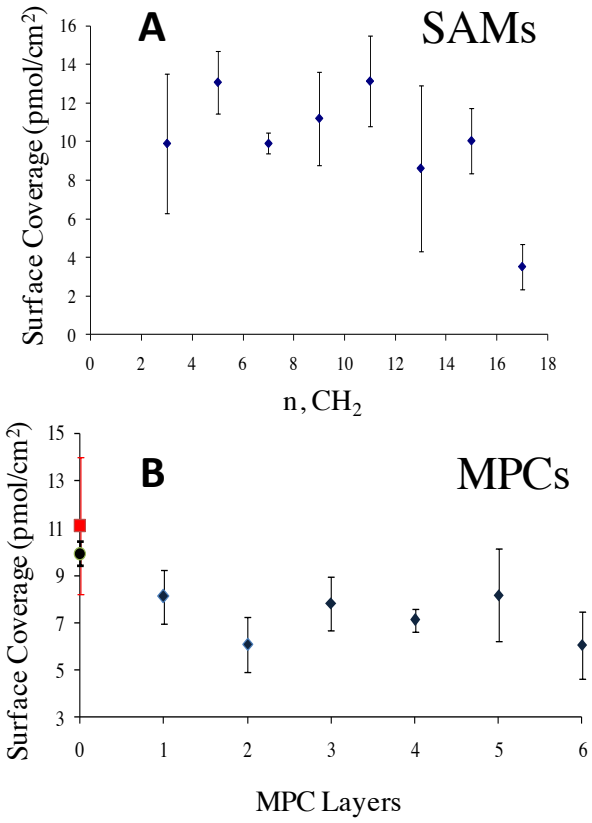

Figure 2. Surface coverage (Γ) comparison for AZ (A) at alkanethiolate SAMs of increasing chainlength (number of methylene units, n) and (B) at MPC film assemblies of increasing thickness (number of MPC layers). For comparison, the average surface coverage of AZ-SAM systems (■) as well as the average coverage of the C8 SAM system (•) are included with the MPC data.

average AZ surface coverage for all the MPC systems was measured at approximately 7.5 $_{(\pm 1.5)}$ pmol/cm^2, with most of the measurements yielding values between 7-9 pmol/cm^2. For comparison on Figure 2B, the average coverage for AZ on all SAM systems, as well as for an individual SAM system (C8), are included. Given the significant thickness of MPC films that

has been previously established[29], minor differences in surface coverage between the two systems is expected, but remains consistent with near monolayer coverage[39].

Similarly, the formal potential (E°´) of AZ at the two different adsorption platforms is compared in **Figure 3**. The lack of distance dependence is evident in the results as there is very little variation in E°´ on the scale presented as the film thickness is increased. Moreover, there is

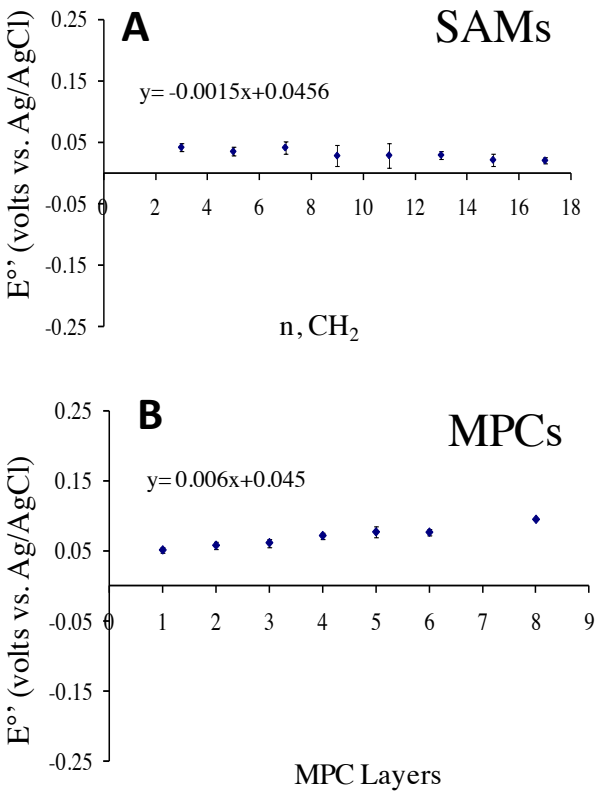

Figure 3. Formal potential (E°´) comparison for AZ (A) at alkanethiolate SAMs of increasing chainlength (number of methylene units, n) and (B) at MPC film assemblies of increasing thicknesses (number of MPC layers). For data points appearing without, error bars, they are smaller than the data marker.

very little standard deviation for individual measured systems with either adsorption platform. The E°´ trends for both systems are clearly linear and suggest nearly the same average (intercept) of +0.045$_3$ V versus the reference electrode. This similarity is encouraging in our comparison

since the MPC films are anchored at the electrode interface with an initial C6 SAM. However, as the films are made thicker and electrode-to-protein distance is increased, there are slightly opposite trends observable in the data. The E°´of AZ at SAMs shows a slight trend toward negative potentials with increasing chainlength whereas AZ at MPC films delineates a shallow ramp toward more positive potentials versus the reference electrode. The exact reason for these opposite, albeit very slight, trends is unknown but it has been previously shown by others [11, 43]that these type of shifts are probably the result of an altered protein environment upon adsorption that induces a differential binding between the oxidized and reduced forms of the protein. Even though the shifts in such reports are significantly larger than those seen in our study, it is feasible that the subtle opposing trends are indeed an indication of the AZ's sensitivity to an adsorption platform that is predominantly hydrophobic thick layer (SAM) versus one with polar metal cores present near the interface region (MPC films). Regardless, the relative distance independence of E°´ in these systems suggests that AZ exists in its native form at each of the adsorption platforms.

Analysis of peak shape in the AZ voltammetry at both adsorption platforms is particularly interesting in these systems. As previously mentioned and identified in PME research of redox proteins, like AZ and cytochrome c, the voltammetric peaks typically display an anomalous broadening that can be quantified by measuring the full-width-at-half-maximum (FWHM) for the redox wave[23]. Ideally and uniformly adsorbed protein monolayers should, in theory, yield voltammetry with a FWHM of ~90 mV[24]. Most PME experiments utilizing SAM platforms, however, result in broadened voltammetric peaks with FWHM values well above the ideal value, typically ranging from 127-170 mV[25, 28]. This phenomena is also observed in our results and is illustrated in **Figure 4A** which tracks FWHM values for AZ

voltammetry at SAMs as a function of increasing chainlength. Of note in the results is the aforementioned trend of larger FWHM values for adsorbed systems, ranging from ~120-130 mV for shorter chain SAMs and an abrupt and dramatic increase in FWHM as the chainlength of the SAM exceeds 11 methylene units. Bowden and coworkers[25] clearly and succinctly identified one source of peak broadening in the voltammetric peaks of PME, utilizing cyt c at hexadecanetholate (C16) SAMs, in that the larger FWHM were the result of a heterogeneous

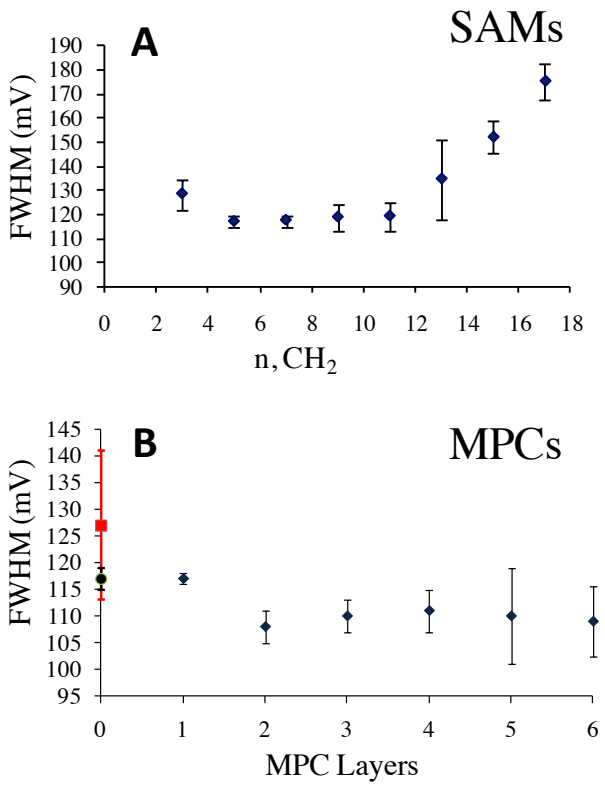

Figure 4. Full-width-at-half-maximum (FWHM) or voltammetric peak broadening for AZ electrochemistry (A) at alkanethiolate SAMs of increasing chainlength (number of methylene units, n) and (B) at MPC film assemblies of increasing thickness (number of MPC layers). For comparison, the average FWHM values of AZ-SAM systems (■) as well as the average FWHM value of the C8 SAM system (●) are included with the MPC data.

population of adsorbed protein that was directly attributed to the lack of uniformity in adsorption microenvironments across the surface[25]. In later reports[23], it was shown that gold substrate topographical features could have a substantial impact on the density of defects in SAMs and

further contribute to the heterogeneity of the protein binding interface[23]. The abrupt increase in FWHM shown in Figure 4A is likely due to a corresponding shift of film structure that occurs with SAMs of varying chainlength that, in turn, makes the adlayer structure more susceptible to topography derived defects that affect the interface. That is, as the number of SAM methylene units increases there is a change in SAM structure, from the more liquid-like interface of shorter chain SAMs to a more rigid, crystalline interface for SAMs comprised of longer chainlengths[41-44]. It follows that the latter films would be more sensitive to translating sources of eventual SAM defects from gold substrate topographical features (e.g., grain boundaries, step edges, plateaus, etc.)[23].

Figure 4B depicts FWHM values for AZ voltammetry where the protein is adsorbed to MPCs films comprised of different numbers of MPC layers. Noticeably absent from this data is the sharp increase in FWHM at thicker films that was observed in the SAM results (Figure 4A). The data also indicates that, as the second layer of MPCs is networked into the film, and likely the first complete MPC coverage of the gold underlayer[28, 29], a corresponding lower FWHM is observed in the voltammetry even without a significant decrease in protein surface coverage (see Figure 2). For comparison purposes, the average FWHM values for all of the SAM systems tested as well as the specific system of C8 SAM are also included as part Figure 4B. After an initial drop with the first two layers of MPCs, the FWHM values appear to level out well below typical SAM values. Whereas some systems did approach (e.g., 100 mV) the FWHM value for ideally adsorbed systems (90 mV), most showed a modest decrease to 100-110 mV after the exposure to six layers of MPCs. For a quantitative comparison, the collective results for measuring the electrochemical properties of AZ at both representative SAM and MPC adsorption platforms are summarized in **Table 1**.

Table 1. Electrochemical Parameters Comparison

	E°' (Volts)	FWHM (mVolts)	Γ (pmol/cm^2)	k°$_{et}$ (s^{-1})
C8 SAM	0.041 (0.010)	118 (2.4)	9.90 (0.539)	14.26 (7.83)
C16 SAM	0.021 (0.002)	152 (6.7)	10.0 (1.67)	0.98 (0.753)
3 Layers MPC	0.061 (0.061)	110 (3.0)	7.81 (1.12)	13.34 (9.45)
5 Layers MPC	0.077 (0.011)	118 (8.2)	8.18 (1.95)	6.07 (2.65)

Note: All MPC film experiments, n = 3-9

Given the establishment of the heterogeneous nature of a SAM interface for protein electrochemistry by Bowden and others[25], our results suggest that MPC layering of the substrate may be a means of improving the homogeneity of protein adsorption sites at an interface, with the surface chemistry of the MPCs in the form of a closely networked film providing a more uniform surface that deemphasizes contributions to film structure originating from gold topographical features. We speculate, as in a prior report[28], that the aforementioned plateau in the data (Figure 4B) may be a sign of a potential limitation of this strategy. Specifically, we believe that inherent polydispersity in the core sizes of MPCs leads to both a high variability film-to-film as well as a limited improvement to the FWHM values observed because of the contributions of polydisperse core sizes being incorporated into the films. To further investigate this possibility, we have extensively studied procedures to decrease the variability of core size in MPC samples that are translated into the film assemblies, including polarity based fractionation procedures as well as ligand exchange "annealing" procedures. The improvement in MPC polydispersity, however, is minimal with little effect on the FWHM values (data not shown).

3.2 Atomic Force Microscopy Analysis of the MPC Film Interface

The results presented suggest that the assembly of an MPC film at a substrate may present a more uniform binding interface for protein adsorption where the microenvironment of adsorption sites, on the scale of a protein, is more consistent over a large surface area. This concept of coating the substrate's surface with a blanket of MPCs was explored with atomic force microscopy (AFM) of gold substrates before and after the assembly of the MPC film. A well-known substrate, gold epitaxially grown on mica features a collection of plateaus, many of which are separated by gold step edges, making it overall one of the more flat substrates for large surface areas available[29,45,46]. In our experiment, gold/mica substrates were cleaned and imaged with AFM prior to the assembly of an MPC film. The three-dimensional AFM generated image presented in **Figure 5A** reflects the typical topography observed for bare gold/mica and is a nice example of the aforementioned flat plateau features. Upon assembly of a 5 layer MPC film at the substrate, care was taken to reimage the same area of the substrate with the MPC film in place. **Figure 5B** represents an AFM image of the topography of the MPC modified gold on mica. From the image, one can easily see that the surface seems homogeneously covered by MPC material, including the prominent large flat plateau centered in the image of Figure 5A. The dramatic change in the surface, from obviously smooth areas that become uniformly filled with topographical roughness (i.e., a "bumpy" appearance), lends support to the idea that MPC films significantly alter the film interface, in turn providing a more homogeneous adsorption environment.

Closer inspection of AFM imaging of the Au-mica substrates before and after the growth of the MPC film assembly reveals evidence that the source of the uniformity may be the

small scale minimization of topographical feature effects. For example, **Figure 6** compares images of the same area of a gold-mica substrate before and after MPC modification of a 5 layer

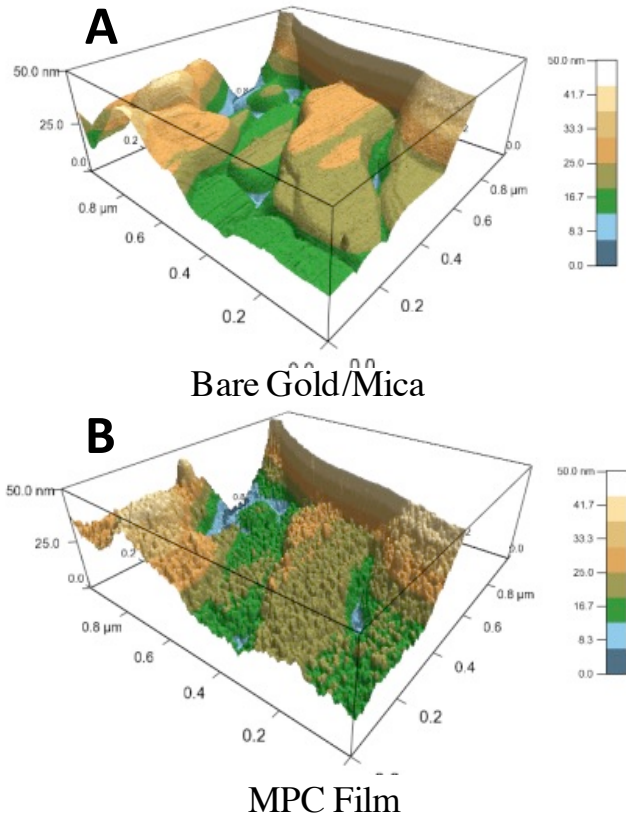

Figure 5. Three dimensional views of AFM images of a gold on mica substrate before (A) and after (B) modification with a five layer MPC film.

film, including cross-sectional analysis of several places on the substrate. We have identified the same area on the substrate before and after the MPC film has been applied by the unique structural feature in the lower left corner of the images (indicated with a black arrowhead in the images). Overall, the images again reveal a significant change in the surface roughness of the flat plateaus upon assembly of the MPC film that are seen in the images of Figure 5. Qualitatively we also see that some of the topographical features that are prominent prior to the MPCs are more "washed out" or obscured by the presence of the MPC film. We highlight two areas (indicated with red circles in the images) where a distinctive surface feature prior to the

MPC film is softened or less sharp in the image after the film is applied. More specifically, cross-sectional analysis of such areas (indicated with the white arrowheads in the images) lends itself to supporting the idea that the MPC film is able to, to some degree, mask certain topographical features. One cross-sectional analysis (Figure 6, 1a→1b) targets a divot or trench in the underlying gold that is approximately 2 nm deep prior to MPC modification and significantly diminished (~0.5 nm depth) after MPC modification. The second feature focus of the cross-sectional analysis is a step edge (Figure 6, 2a→2b) approximately 3 nm in height and a

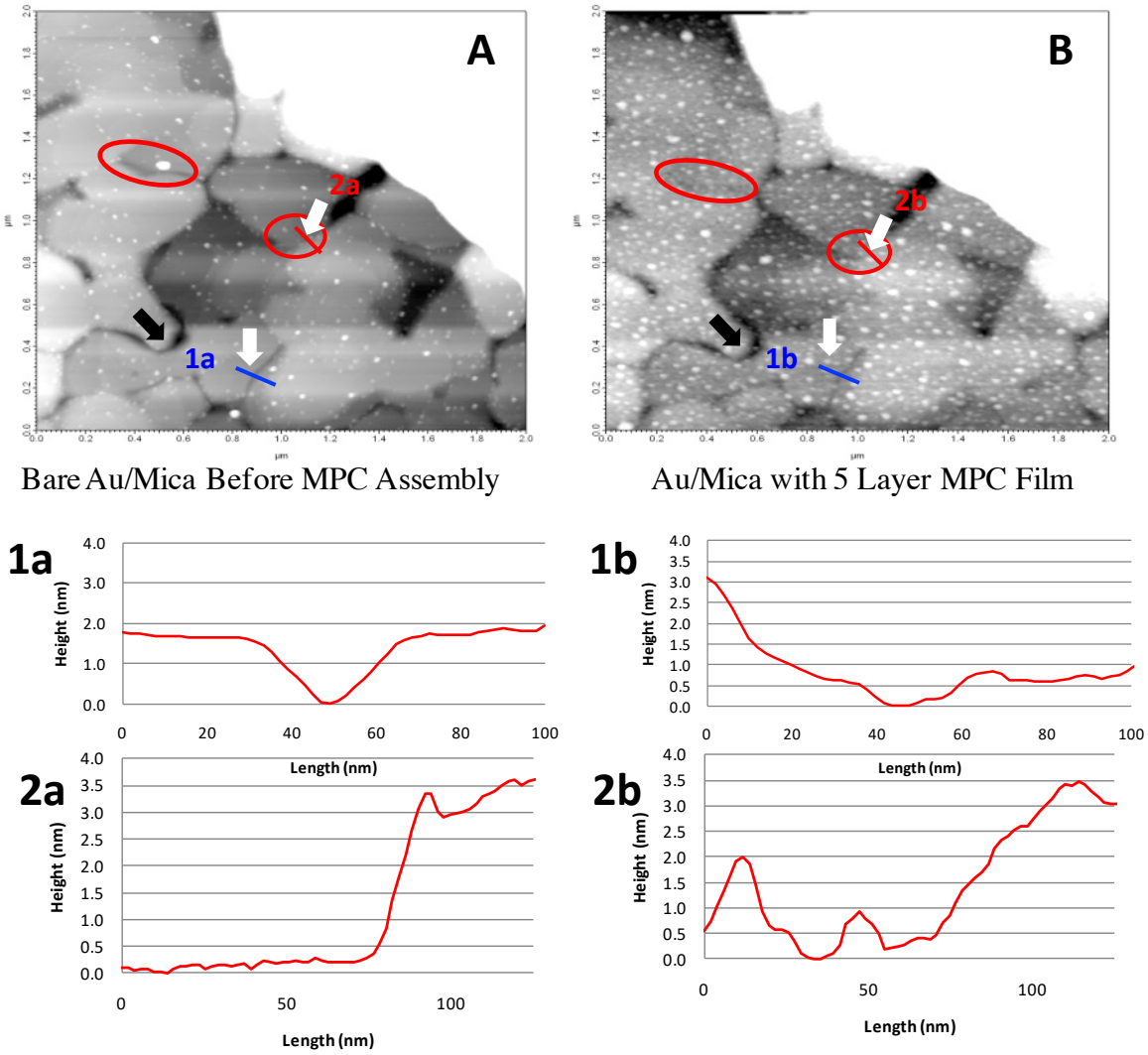

Figure 6. AFM image of the same area of a gold mica substrate, identified by the unique feature marked with the black arrowhead, before (A) and after (B) modification with a 5 layer MPC film. Both simple visual (red circles) and cross sectional analysis (white arrowheads) are also included for a shallow trench (1a → 1b) as well as sharp step edge (2a → 2b) before and after assembling the MPC film. Note: Additional information on AFM imaging and cross-sectional analysis of the substrate is included in the Supporting Materials.

nearly vertical incline. After the application of an MPC film, the transition is more sloped, not nearly as sharp. Additionally, the cross-sectional analysis (Figure 6-2b) reveals the MPC-treated substrate exhibits additional features to the left of the step edge. These features are consistent with the imaging results of Figure 5 where even the topography of the gold's flat terraces becomes altered upon modification with a MPC film. Collectively, the AFM imaging results suggest that the MPC films may be functioning to both "blur" the gold topographical features that are known to contribute to SAM defect density and uniformly coating the surface with a material that, regardless of orientation[31], is presenting a similar adsorption environment on the scale of a protein. If these effects are widespread, across large areas of the surface, it follows that proteins adsorbed to such surfaces would experience more homogeneous adsorption interactions and an overall lowering of the heterogeneity of the interface.

3.3 Systematic Desorption Studies of AZ Electrochemistry

Bowden and coworkers provided evidence of a heterogeneous population of adsorbed proteins through a set of systematic desorption experiments[25]. Using a monolayer of cyt c adsorbed electrostatically to carboxylic acid SAMs that were subsequently desorbed with exposure to increasing ionic strength washes, Bowden was able to track the electrochemical properties, including formal potential (E°´), FWHM, and ET rate constant (k_{ET}°), of different populations of adsorbed protein. As the more weakly bound protein was removed via systematic desorption, the remaining strongly bound protein exhibited more negative E°´, smaller FWHM values, and faster k_{ET}°, most likely the result of these proteins being adsorbed in more optimal environments. This work established the heterogeneous adsorption environments of cyt c being

directly related to the inherent peak broadening observed in PME as the result of slight variation of adsorption sites causing variation in the measured electrochemical parameters[25].

Here, we apply a similar desorption strategy to our AZ systems. Unlike Bowden's work with cyt c, however, AZ binds to the SAM or MPC films via a hydrophobic interaction versus the electrostatic adsorption[19]. Requiring a different systematic desorption strategy, we first explored simple rinsing of AZ at SAMs with UP water to remove the weakly bound protein. Desorption with water rinsing was only partially successful, unable to completely remove a significant portion of adsorbed protein. Eventually, the systematic desorption to this population of water resistant, strongly bound AZ at SAMs did indeed show a corresponding trend toward smaller FWHM values, for example (Supporting Materials). However, since the water rinsing was unable to remove a significant portion of the protein we explored alternative desorption strategies.

More effective desorption of AZ from SAMs was accomplished by introducing an organic modifier into the washing protocol, namely the percent ethanol concentration was systematically increased from 5% to 30% (v/v) during each successive desorption rinse. During each rinse, the cell was filled with the ethanol solution for one minute then rinsed (5x) with potassium phosphate buffer in preparation for electrochemical analysis. Control experiments such as UV-Vis and fluorescence spectroscopy were carried out by treating solutions of AZ with 30% (v/v) ethanol and revealed no evidence of protein denaturation at this ethanol concentration even after 3 days of exposure (Supporting Materials). Additionally, electrochemical investigations of the SAMs, including capacitance measurements and linear sweep electrochemical desorption of the alkanethiolates, before and after the ethanol-water rinsing treatment indicated that very little SAM damage was occurring (Supporting Materials). **Figure 7**

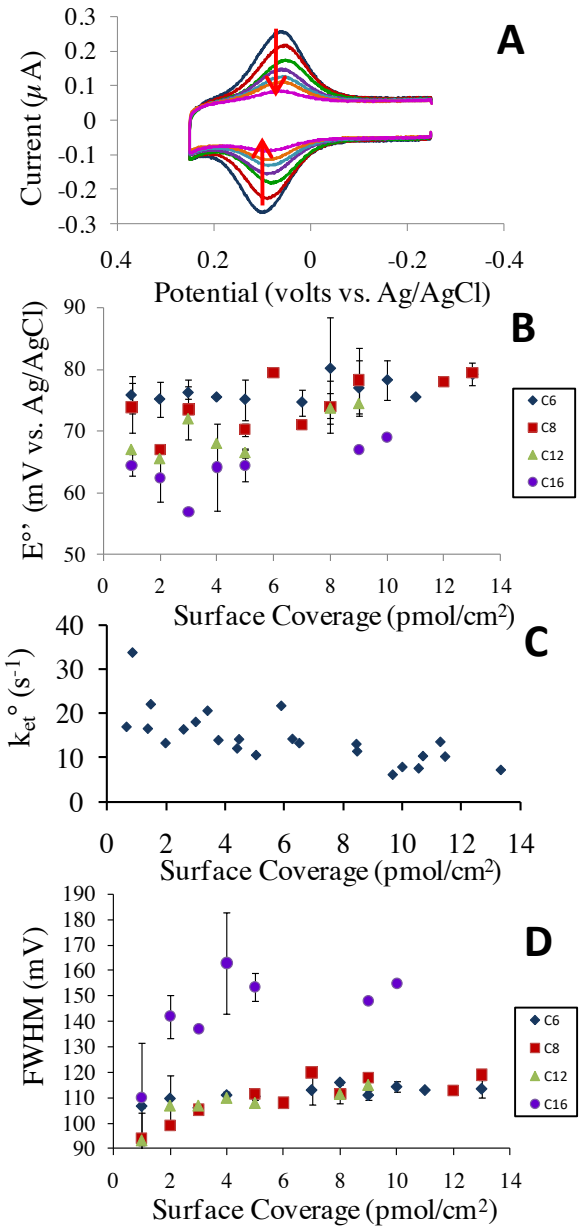

Figure 7. (A) An example of cyclic voltammetry for AZ monolayer at a C8 SAM during systematic desorption of the protein with solutions of increasing ethanol concentrations (5%→ 30% v/v) along with desorption tracking of electrochemical parameters including (B) formal potential (E°´), (C) ET rate constant ($k_{et}°$) (C8 SAM only), and (D) FWHM values for AZ at SAM of various chainlengths.

tracks the results for ethanol desorption of AZ from SAMs of varying chainlengths. Our results on SAMs during the desorption of AZ echo the same trends observed by Bowden in that as the more strongly bound protein is systematically isolated (decreasing surface coverage), there is a

corresponding shift of E°′ to more negative potentials (Figure 7B), faster $k_{ET}°$ (Figure 7C) and lower FWHM values (Figure 7D). Inherent in the results is also distinctive chainlength dependent trends where the aforementioned shifts in electrochemical parameters are more dramatic, most notably FWHM, for SAMs of longer chainlength (C6 vs. C16 SAMs, for example). The observed chainlength trends are likely due to the structural transition of shorter chain versus longer chain SAMs, where the more crystalline structure of the latter assists in isolating different types of adsorption sites (compared to the more fluid-like interface of short chain SAMs)[41-44].

If modification of an interface with a MPC film indeed improves the homogeneity of adsorption sites for AZ, the trends observed with SAMs should be less pronounced at MPC films. Indeed, if the MPC films provide a more uniform adsorption environment, one would expect AZ desorption to not proceed in the stepwise manner seen at SAMs with respect to the electrochemical parameters and, alternatively, should exhibit less substantial or no trends at all. **Figure 8** shows the desorption of AZ at a 5 layer MPC film in comparison to a relatively short chain (C8) SAM. Even compared to a short chain SAM which displayed less pronounced changes in the electrochemical parameters in Figure 7, desorption from MPC films does not yield the same trends. Instead, we observe very little change in FWHM, a key indicator of heterogeneous adsorption sites for protein, or $k_{ET}°$ which is observed to be between 5-10 sec^{-1} regardless of the desorption. The typically observed trend in E°′ shifting to more negative potentials for AZ desorption at SAM platforms, a nearly 15 mV decrease (Figure 7B), is not observed with the same experiments at MPC films[47]. Overall, while not dramatic, the cumulative results of our desorption experiments do supply additional evidence suggesting that MPC films provide a more homogeneous adsorption interface for the redox protein AZ.

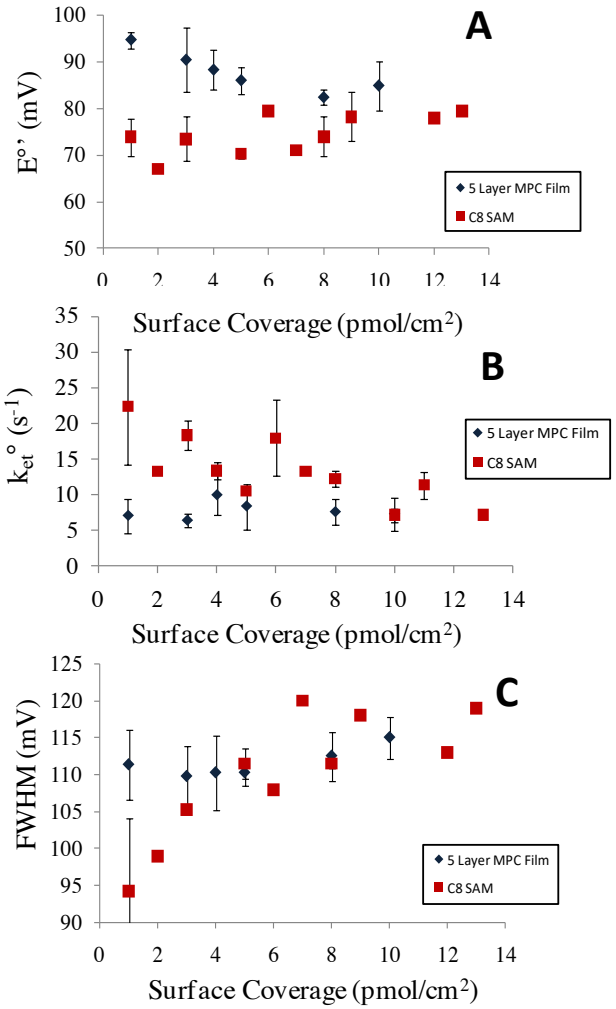

Figure 8. Desorption tracking of electrochemical parameters for AZ at 5 Layer MPC film and C8 SAM with increasing ethanol concentrations (5% → 30% v/v). A) Formal potential B) Electron transfer kinetics ($k_{et}°$) C) FWHM values.

3.4 Application of MPC Films to Protein Resistant Platforms

One application for the homogeneous MPC interface is as use as an adaptation to transform films that are resistant to protein immobilization into more effective adsorption platforms. As previously indicated, AZ adsorbs via a hydrophobic interaction at a substrate, in our study, for instance, this is a methyl-terminated SAM or a C6 protected nanoparticle film. In contrast, our results show that there is virtually no adsorption of AZ at hydrophilic, carboxylic acid terminated SAMs. To test the aforementioned application of the MPC films, SAMs

comprised of only carboxylic acid thiolates were assembled and subsequently further modified with layers of MPC via dithiol linkages. As shown in **Figure 9**, by augmenting the protein resistant SAMs like MUA with an MPC film assembly, one is able to effectively induce AZ adsorption and electrochemistry. Even with the increased capacitance or non-Faradaic background signal that accompanies the use of the MPCs[28], the insertion of the nanoparticle film and the regeneration of AZ adsorbed electrochemistry is clearly evident. Similar results were achieved at SAMs of MHA with the use of NDT to anchor and network an MPC film at that interface prior to the adsorption of AZ. Control experiments on the protein resistant SAMs before and after the exposure to solutions of dithiol linkers confirm that there is very little displacement of the original carboxylic acid terminated alkanethiolates and suggest that the MPC film is indeed assembled on top of the SAM (Supporting Materials). This set of experiments further demonstrates the interfacial control available from the use of MPC films that are employed for a specific outcome.

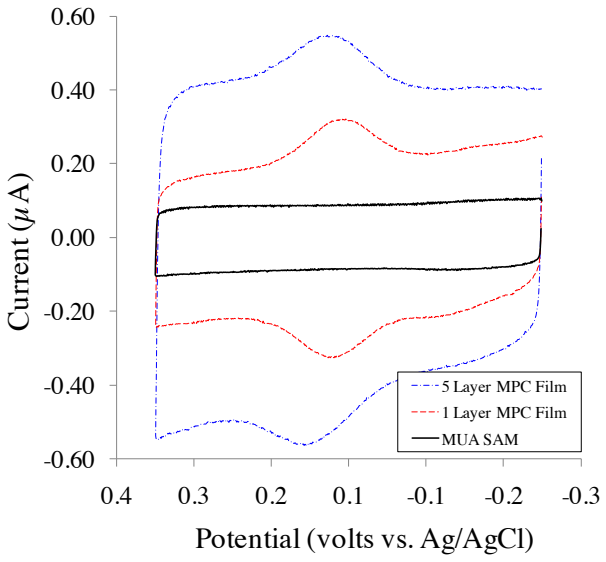

Figure 9. Cyclic voltammetry of AZ monolayers at a MUA SAM and at MUA SAMs subsequently modified with 1 and 5 layer hexadecanedithiol-linked MPC film assemblies. Similar results were achieved at a MHA SAM (Supporting Materials).

Conclusion

The traditional SAM-modified electrode strategy for PME is inherently limited in its success due to a lack of molecular level control of the interface, a factor that results in heterogeneous adsorption environments for protein immobilization and, in turn, a broadened voltammetric signal that deviates from established theory. The most significant finding of this work is that greater interfacial control of the protein-substrate interface may be achieved with the use of MPC film assemblies that coat the interface and provide a more uniform adsorption environment. Confirmation of improved molecular level control of the adsorption interface is surmised from shifts of key electrochemical parameters such as FWHM while maintaining near monolayer surface coverage and stable formal potentials. The use of MPC film assemblies in this manner is justified by our ability to use electrochemistry and microscopy to show that the underlying gold topography and adlayer sub-structure that normally influences traditional SAM-based platforms can be effectively masked and that MPCs offer a more homogeneous display of interfacial interactions for protein immobilization over a large surface area. These two factors ultimately results in a more singular population of adsorbed protein that is a direct consequence of greater control of protein nanoscale adsorption environment, identified as a key factor in understanding protein-electrode coupling schemes.[28, 48-50]

Acknowledgements

We gratefully acknowledge the National Science Foundation generously supporting this research (CHE-0847145). Additionally, MLT acknowledges that this research was partially supported by the American Chemical Society Petroleum Research Fund (46380-GB7). We are also grateful to Carolyn Marks (University of Richmond, Biology) for helping us with the TEM imaging and to Debbie Campbell-Rance, Michael Freeman, and Natalie Nguyen for their contributions to this work. Special thanks is given to Drs. Rene Kanters, Diane Kellogg, Rob Miller and Will Case, as well as Russ Collins, Phil Joseph, Mandy Mallory, and John Wimbush - all of whom make undergraduate research possible at the University of Richmond. A personal thank you is given to Tammy for her support over the years.

Supporting Information Available:

Double-layer capacitance tracking for SAMs; AFM images; AZ desorption with water results; UV-Vis and fluorescence of AZ in EtOH; Liner sweep voltammetry and double –layer capacitance of SAM after AZ desorption; Cyclic voltammetry of AZ at MHA SAMs modified with MPC films.

Captions

Figure 1. Cyclic voltammograms (100 mV/sec) of azurin monolayers adsorbed to a C6 SAM (solid line, red) and a three layer MPC film composed of $Au_{225}C6_{75}$ (dotted line, blue). Inset: Schematic representations of the systems investigated in this study. [Protein monolayer electrochemistry solution conditions: 4.4 mM potassium phosphate buffer, pH=7, μ=10 mM]

Figure 2. Surface coverage (Γ) comparison for AZ (A) at alkanethiolate SAMs of increasing chainlength (number of methylene units, n) and (B) at MPC film assemblies of increasing thickness (number of MPC layers). For comparison, the average surface coverage of AZ-SAM systems (■) as well as the average coverage of the C8 SAM system (•) are included with the MPC data.

Figure 3. Formal potential (E°´) comparison for AZ (A) at alkanethiolate SAMs of increasing chainlength (number of methylene units, n) and (B) at MPC film assemblies of increasing thicknesses (number of MPC layers). For data points appearing without, error bars, they are smaller than the data marker.

Figure 4. Full-width-at-half-maximum (FWHM) or voltammetric peak broadening for AZ electrochemistry (A) at alkanethiolate SAMs of increasing chainlength (number of methylene units, n) and (B) at MPC film assemblies of increasing thickness (number of MPC layers). For comparison, the average FWHM values of AZ-SAM systems (■) as well as the average FWHM value of the C8 SAM system (•) are included with the MPC data.

Figure 5. Three dimensional views of AFM images of a gold on mica substrate before (A) and after (B) modification with a five layer MPC film.

Figure 6. AFM image of the same area of a gold mica substrate, identified by the unique feature marked with the black arrowhead, before (A) and after (B) modification with a 5 layer MPC film. Both simple visual (red circles) and cross sectional analysis (white arrowheads) are also included for a shallow trench (1a → 1b) as well as sharp step edge (2a → 2b) before and after assembling the MPC film. Note: Additional information on AFM imaging and cross-sectional analysis of the substrate is included in the Supporting Materials.

Figure 7. (A) An example of cyclic voltammetry for AZ monolayer at a C8 SAM during systematic desorption of the protein with solutions of increasing ethanol concentrations (5%→ 30% v/v) along with desorption tracking of electrochemical parameters including (B) formal potential (E°´), (C) ET rate constant (k_{et}°) (C8 SAM only), and (D) FWHM values for AZ at SAM of various chainlengths.

Figure 8. Desorption tracking of electrochemical parameters for AZ at 5 Layer MPC film and C8 SAM with increasing ethanol concentrations (5% → 30% v/v). A) Formal potential B) Electron transfer kinetics (k_{et}°) C) FWHM values.

Figure 9. Cyclic voltammetry of AZ monolayers at a MUA SAM and at MUA SAMs subsequently modified with 1 and 5 layer hexadecanedithiol-linked MPC film assemblies. Similar results were achieved at a MHA SAM (Supporting Materials).

References

[1] W.H. Scouten, J.H. Luong, R.S. Brown, Trends in Biotechnology. 13 (1995) 178-185.

[2] K.L. Davis, B.J. Drews, H. Yue, D.H. Waldeck, K. Knorr, R.A. Clark, J Phys Chem C. 112 (2008) 6571.

[3] G. Ramsay (Ed.), Commercial Biosensors - Applications to Clinical, Bioprocess, and Environmental Samples, John Wiley & Sons, Inc., New York, 1998.

[4] A.L. Ghindilis, P. Atanasov, E. Wilkins, Biosensors and Bioelectronics. 13 (1998) 113.

[5] J. Nam, T.C. Shad, C.A. Mirkin, Science. 301 (2003) 1884.

[6] E.F. Bowden, Electrochemical Society Interface. 6 (1997) 40.

[7] N.A. Stasko, M.H. Schoenfisch, J Am Chem Soc. 128 (2006) 8265.

[8] M. Mrksich, G.M. Whitesides, Annu Rev Biophys Biomol Struct. 25 (1996) 55.

[9] A. Heller, J. Phys. Chem. 96 (1992) 3579-3587.

[10] F.A. Armstrong, H.A.O. Hill, N.J. Walton, Acc Chem Res. 21 (1988) 407-413.

[11] J.L. Willit, E.F. Bowden, J Phys Chem. 94 (1990) 8241.

[12] E.A.E. Garber, E. Margoliash, Biochimica et Biophysica Acta, Bioenergetics. 1015 (1990) 279.

[13] E.F. Bowden, R.A. Clark, J.L. Willit, S. Song, Proceedings - Electrochemical Society. 93-11 (1993) 34.

[14] S. Song, R.A. Clark, E.F. Bowden, M.J. Tarlov, J Phys Chem. 97 (1993) 6564.

[15] K. Nakano, T. Yoshitake, Y. Yamashita, E.F. Bowden, Langmuir. 23 (2007) 6270.

[16] A. Avila, B.W. Gregory, K. Niki, T.M. Cotton, J Phys Chem B. 104 (2000) 2759.

[17] K. Niki, W.R. Hardy, M.G. Hill, H. Li, J.R. Sprinkle, E. Margoliash, K. Fujita, R. Tanimura, N. Nakamura, H. Ohno, J.H. Richards, H.B. Gray, J Phys Chem B. 107 (2003) 9947.

[18] B.D. Fleming, S. Praporski, A.M. Bond, L.L. Martin, Langmuir. 24 (2008) 323.

[19] Q. Chi, J. Zhang, J.E.T. Andersen, J. Ulstrup, J Phys Chem B. 105 (2001) 4669.

[20] K. Fujita, N. Nakamura, H. Ohno, B.S. Leigh, K. Niki, H.B. Gray, J.H. Richards, J Am Chem Soc. 126 (2004) 13954.

[21] K. Yokoyama, B.S. Leigh, Y. Sheng, K. Niki, N. Nakamura, H. Ohno, J.R. Winkler, H.B. Gray, J.H. Richards, Inorg Chim Acta. 361 (2008) 1095.

[22] R.J. Cherry, A.J. Bjornsen, D.C. Zapien, Langmuir. 14 (1998) 1971.

[23] M.C. Leopold, E.F. Bowden, Langmuir. 18 (2002) 2239.

[24] A.J. Bard, L.R. Faulkner, Electrochemical Methods Fundamentals and Applications, John Wiley & Sons, New York, 1980.

[25] R.A. Clark, E.F. Bowden, Langmuir. 13 (1997) 559-565.

[26] M. Niemeyer, Angew Chem Int Ed Engl. 40 (2001) 4128.

[27] K. Kerman, M. Saito, E. Tamiya, S. Yamamura, Y. Takamura, TrAC, Trends Anal Chem. 27 (2008) 585.

[28] A.F. Loftus, K.P. Reighard, S.A. Kapourales, M.C. Leopold, J Am Chem Soc. 130 (2008) 1649.

[29] M.L. Vargo, C.P. Gulka, J.K. Gerig, C.M. Manieri, J.D. Dattelbaum, C.B. Marks, N.T. Lawrence, M.L. Trawick, M.C. Leopold, Langmuir. 26 (2010) 560.

[30] M. Brust, M. Walker, D. Bethell, D.J. Schriffrin, R.J. Whyman, J Chem Soc - Chem Commun. (1994) 801.

[31] A.C. Templeton, W.P. Wuelfing, R.W. Murray, Acc Chem Res. 33 (2000) 27.

[32] M. Collinson, E.F. Bowden, M.J. Tarlov, Langmuir. 8 (1992) 1247.

[33] J.C. Hoogvliet, M. Dijksma, B. Kamp, W.P. van Bennekom, Anal Chem. 72 (2000) 2016.

[34] E. Laviron, J Electroanal Chem. 101 (1979) 19.

[35] J.F. Hicks, F.P. Zamborini, R.W. Murray, J Phys Chem B. 106 (2002) 7751.

[36] P.S. Jensen, Q. Chi, F.B. Grumsen, J.M. Abad, A. Horsewell, D.J. Schiffrin, J. Ulstrup, Journal of Physical Chemistry C. 111 (2007) 6124.

[37] B. Rizzuti, V. Daggett, R. Guzzi, L. Sportelli, Biochemistry (N Y). 43 (2004) 15604.

[38] H.O. Finklea, Electroanalytical Chemistry. 19 (1996) 109.

[39] A.K. Gaigalas, G. Niaura, J Colloid Interface Sci. 193 (1997) 60.

[40] J. Petrovic, R.A. Clark, H. Yue, D.H. Waldeck, E.F. Bowden, Langmuir. 21 (2005) 6308.

[41] C.D. Bain, E.B. Troughton, Y.T. Tao, J. Evall, G.M. Whitesides, R.G. Nuzzo, J Am Chem Soc. 111 (1989) 321.

[42] S.J. Stranick, A.N. Parikh, Y.-. Tao, D.L. Allara, P.S. Weiss, J Phys Chem. 98 (1994) 7636.

[43] P.E. Laibinis, R.G. Nuzzo, G.M. Whitesides, J Phys Chem. 96 (1992) 5097.

[44] S.V. Atre, B. Liedberg, D.L. Allara, Langmuir. 11 (1995) 3882.

[45] C.R. Clemmer, T.P. Beebe, Scanning Microscopy. 6 (1992) 319.

[46] D.J. Trevor, C.E.D. Chidsey, D.N. Loiacono, Physical Review Letters. 62 (1989) 929.

[47] Sytematic desorption of AZ from MPC films results in a nearly 10 mV increase in E°´. The reason for the opposite shift in E°´ is currently not well understood.

[48] P. Asuri, S.S. Karajanagi, H. Yang, T. Yim, R. Kane S., J. Dordick S., Langmuir. 22 (2006) 5833-5836.

[49] H. Yue, D. Khoshtariya, D.H. Waldeck, J. Grochol, P. Hildebrandt, D.H. Murgida, J Phys Chem B. 110 (2006) 19906.

[50] P. Roach, D. Farrar, C.C. Perry, J Am Chem Soc. 128 (2006) 3939-3945.